Competition between Photochemistry and Energy Transfer in UV-Excited Diazabenzenes. 4. UV Photodissociation of 2,3-, 2,5-, and 2,6-Dimethylpyrazine

Andrew M. Duffin,[†] Jeremy A. Johnson,[‡] Mark A. Muyskens,[§] and Eric T. Sevy*

Department of Chemistry and Biochemistry, Brigham Young University, Provo, Utah 84602

Received: August 3, 2007; In Final Form: September 20, 2007

The quantum yield for HCN formation via 248 nm photodissociation of 2,3-, 2,5-, and 2,6-dimethylpyrazine (DMP, $C_6N_2H_8$) was measured using diode laser probing of the HCN photoproduct. The total quantum yield is $\phi = 0.039 \pm 0.07$, 0.14 ± 0.02, and 0.30 ± 0.06 for 248 nm excitation of 2,3-, 2,5- and 2,6-DMP, respectively. Analysis of the quenching data within the context of a gas kinetic, strong collision model allows an estimate of the rate constant for HCN production via DMP photodissociation, $k_s = 4.1 \times 10^3$, 1.0×10^3, and 1.3×10^4 s^{-1} for 2,3-, 2,5- and 2,6-DMP, respectively. Unlike HCN produced from the photodissociation of pyrazine and methylpyrazine, the amount of HCN produced via a prompt, unquenched dissociation channel was essentially zero, suggesting little multiphoton UV absorption. The rate constants for HCN formation together with previously measured rate constants for HCN production from photodissociation of pyrazine and methylpyrazine have been used to investigate possible reaction mechanisms. The position of the methyl group affects the HCN rate constant, suggesting that the mechanism for pyrazine dissociation involves an initial step that is hindered by the addition of the methyl groups. The proposed initial molecular motion of the mechanism, an out-of-plane H atom migration across a N atom, is consistent with (1) the position of the methyl groups, (2) the dissociation lifetime of the various pyrazine molecules studied, and (3) the observed large energy transfer magnitudes from pyrazine near dissociation. These so-called "supercollisions" have been linked to low-frequency, out-of-plane motion, suggesting that the molecular motions leading to efficient energy transfer are the same motions involved in dissociation. In addition, the pyrazine ($C_4N_2H_4$) 248 nm photoproduct (C_3H_3N) was identified as acrylonitrile using IR spectroscopy, an observation that aids in understanding the dissociation mechanism.

I. Introduction

Researchers have long understood that collisional energy transfer processes and chemical reactions are closely related.[1] For example, in unimolecular reactions the rate of product formation involves not only the rate constant for the reactive step but also rate constants for both collisional activation and deactivation processes.[2] Thus the competition and relationship between reaction and energy transfer is critical to a complete understanding of either process.

In recent years, studies of energy transfer processes have focused, in particular, on understanding the energy transfer probability distribution function, $P(E,E')$.[3−15] This function describes the probability that a molecule initially at energy E' will, following a single collision event, have an energy E. A great deal of effort in energy transfer studies has also been expended to understand the role of "supercollisions",[13−52] events in which a large amount of energy is transferred is a single collision, in relaxation processes.

Clary, Gilbert, Bernshtein, and Oref[27] have put forward a "mechanism" for supercollisions involving highly vibrationally excited donor molecules and a monatomic bath. The results of their vibrational close-coupling, infinite-order sudden approximation quantum-scattering (VCC-IOSA) calculations indicate that low-frequency, particularly out-of-plane, vibrational motion of the donor molecule is primarily responsible for these so-called supercollisions. In particular, their results indicate that only the three lowest frequency benzene vibrational modes result in large amounts of energy transfer; the most efficient energy transfer mode being both low in frequency and out-of-plane in character. Even when the frequency of in-plane vibrational modes is artificially altered to be the same as the out-of-plane mode, the energy transfer efficiency of the out-of-plane mode is still more efficient.

Lendvay,[33] in his classical trajectory study of collisional energy transfer from vibrationally excited CS_2 made the same observation; both frequency and mode character are responsible for efficient collisional energy transfer. He referred to the modes involved in energy transfer as "conduits" through which energy "leaks out" of the donor into the bath molecule. Other, non-gateway modes, only become active in the energy transfer process when their vibrational frequency is artificially lowered and the vibrational frequency of the gateway modes is increased. Simply lowering the frequency of the non-gateway modes does not make them as efficient as the gateway modes.

Recent work in our lab[53] suggests that there is a significant change in both $P(E,E')$ and the average energy transfer, $\langle \Delta E \rangle$, for the pyrazine/CO_2 system as the pyrazine internal energy approaches the threshold energy for pyrazine unimolecular dissociation. In particular, we observed a sharp increase in $\langle \Delta E \rangle$

* Author to whom correspondence should be sent. E-mail: esevy@byu.edu. Phone: 801-422-7235. Fax: 801-422-0153.

[†] Present address: Department of Chemistry, University of California—Berkeley, Berkeley, CA 94720.

[‡] Present address: Department of Chemistry, Massachusetts Institute of Technology, Cambridge, MA 02139.

[§] Permanent address: Department of Chemistry and Biochemistry, Calvin College, Grand Rapids, MI 49546.

10.1021/jp0762471 CCC: $37.00
Published on Web 11/30/2007

and in the "fraction" of strong (i.e., super) collisions (from 1.2 to 5.4%) in a 500 cm^{-1} range near the dissociation energy of pyrazine. These observations are corroborated by classical trajectory calculation of SO_2 relaxation by Lendvay, Schatz, and Harding.[28] They observed that $\langle\Delta E\rangle$ increases nearly linearly with an increase in SO_2 internal energy until the internal energy approaches the dissociation threshold; at this point, the dependence of $\langle\Delta E\rangle$ on $\langle E\rangle$ becomes stronger than quadratic. Although it is expected that increasing internal energy should increase the amount of energy transferred, leading to changes in $P(E,E')$, it is initially surprising that the effect is so dramatic. Based on our results, the dramatic increase in $\langle\Delta E\rangle$ in the energy region near threshold is due almost entirely to the increasing fraction of strong collisions.

The existence of gateway modes for large energy transfer events and the relationship between the fraction of strong collisions, $\langle\Delta E\rangle$, and internal energy suggest that the vibrational modes responsible for "supercollisions" are the same modes that couple into the reaction coordinate for the dissociation process. Hence, as internal energy increases, the low-frequency, out-of-plane vibrational modes responsible for supercollisions are excited with more and more quanta of energy, such that these large amplitude modes lead to efficient collisional energy transfer and unimolecular reaction along a reaction coordinate related to that vibrational "gateway" mode. To test this idea, we present here continued work on the 248 nm photodissociation of pyrazine.[51,52,54,55] The purpose of the experiments described here is 2-fold. First, determine the rate constant for 248 nm photodissociation of the dimethylpyrazines as has been studied previously with pyrazine[52,54] and methylpyrazine,[55] and second, use the HCN quantum yields and formation rate constant, along with the results from pyrazine and methylpyrazine dissociation, to test the viability of pyrazine dissociation mechanisms and the potential relationship of those mechanisms to energy transfer processes involving pyrazine. Specifically, we are interested in determining if potential unimolecular reaction pathways are consistent with energy transfer mechanisms of Clary et al. and Lendvay, which would suggest that the molecular motions leading to unimolecular dissociation are the same motions responsible for large energy transfer events.

II. Experimental Methods

A. Classical Quenching Studies of Dimethylpyrazine Photodissociation. The experimental technique for determining quantum yields has been described previously[52,54,55] and will only be briefly outlined here. A closed 3 m Pyrex cell containing gas-phase samples of 2,3-, 2,5-, or 2,6-dimethylpyrazine are excited by 40−100 UV laser pulses from a KrF excimer laser (Lambda Physik EMG 201, 15 ns pulse width) at 248 nm and 1 Hz. The number of shots is sufficient to produce measurable amounts of photoproduct without depleting the sample. Laser intensities are kept low to avoid multiphoton absorption, 9.8, 6.6, and 7.4 mJ/cm^2 for 2,3-, 2,5-, and 2,6-DMP, respectively. Experiments are conducted at a number of DMP pressures from 1 to 1000 mTorr. The collimation of the ca. 1.5 cm diameter beam is adjusted to ensure that the UV beam emerges from the cell unattenuated by the 2.5 cm diameter cell aperture, and the beam is turned with a 248 nm coated dichroic mirror onto a joulemeter detector (Gentec, ED-200), which gives 10.5 mV/mJ response at these wavelengths. Typically, the peak height from the UV signal is determined by averaging 40−100 laser pulses with a digital oscilloscope (LeCroy 9354A).

The amount of HCN photoproduct is measured by infrared absorption using an IR diode laser technique.[56] A continuous wave (cw), 3.1 μm diode laser beam (Mütek) propagates collinearly with the UV beam through the cell and passes through a monochromator (Bausch & Lomb, 0.5 m) to select a single diode laser mode. The diode laser controller (Laser Analytics) modulates the laser frequency over the entire P19 (or P20) 00°0 → 00°1 absorption line of HCN at 1 kHz, and the central diode laser frequency is actively locked using a technique described below. The digital oscilloscope records the amplified signal from a liquid nitrogen cooled InSb detector (Santa Barbara Research Center) placed at the exit slit of the monochromator. A dual-channel acquisition technique[30] is used to compensate for diode laser intensity fluctuations, and the result from the summed-average of 1000 sweeps across the absorption line is stored. This signal is usually acquired several minutes after the UV exposure is complete to allow for equilibration of the cell contents. Variations in diode laser power across the absorption line are corrected for by subtracting the IR signal obtained from an empty cell from the absorption signals obtained from a cell filled with sample.

Active locking of the diode laser frequency to an HCN absorption line is accomplished using a separate HCN reference cell.[57] A 30 cm long Pyrex reference cell filled with 1,3,5-triazine is irradiated with 248 nm excimer laser pulses, thus producing HCN via 1,3,5-triazine photodissociation.[58,59] Approximately ten percent of the diode laser beam is directed by a beamsplitter into the reference cell, through a monochromator (Instruments SA Inc., HR-320), and then focused onto an InSb detector (Santa Barbara Research Center) followed by a high-gain preamplifier. The HCN IR absorption signal from the reference detector is input to a lock-in amplifier (Princeton Applied Research, Model 117), the output of which is used as an error signal sent to the diode laser controller, thus keeping the diode laser frequency locked to the HCN absorption transition.

UV absorption measurements of the dimethylpyrazine molecules is monitored as a function of total pressure.[60] Linearity of UV absorbance as a function of dimethylpyrazine pressure is used as a quality check of the data.

B. Studies of Pyrazine C_3H_3N Photoproduct. For studies of the C_3H_3N pyrazine photoproduct, a Bruker IFS-66 FTIR equipped with a LN2 cooled MCT detector was used to collect a complete infrared spectrum of the pyrazine photoproducts following 248 nm irradiation. A 10 cm Pyrex cell with CaF_2 widows was filled with 10−20 mTorr of pyrazine. Pyrazine in the cell was exposed to several hundred shots from a 248 nm excimer laser (Lambda Physik Compex 201) with a laser intensity of 6−10 mJ/cm^2. UV absorbance was monitored to determine when the majority of pyrazine was dissociated. Once there was only minimal UV absorbance, the excimer laser was stopped. The cell was then placed in the FTIR and the infrared spectrum was collected. The cell was evacuated of contents and the same cell was used to collect an IR spectrum of a 10−20 mTorr sample of acrylonitrile.

The same cell was used to collect a UV absorption spectrum of the pyrazine photoproducts using a Cary 5E UV−vis-NIR spectrophotometer. The same procedure was followed to create photoproducts for these studies as for the FTIR signals. Again, the cell contents were evacuated and the UV−vis−NIR spectrometer was used to collect a UV spectrum of acrylonitrile.

C. Samples. 2,3-, 2,5-, 2,6-, dimethylpyrazine, and acrylonitrile (Aldrich, 99%, 98%, 98%, and 99+%, respectively) were purified by several freeze (77 K)/pump/thaw cycles. Gas pressures in the cell were monitored with a 1 Torr (MKS-

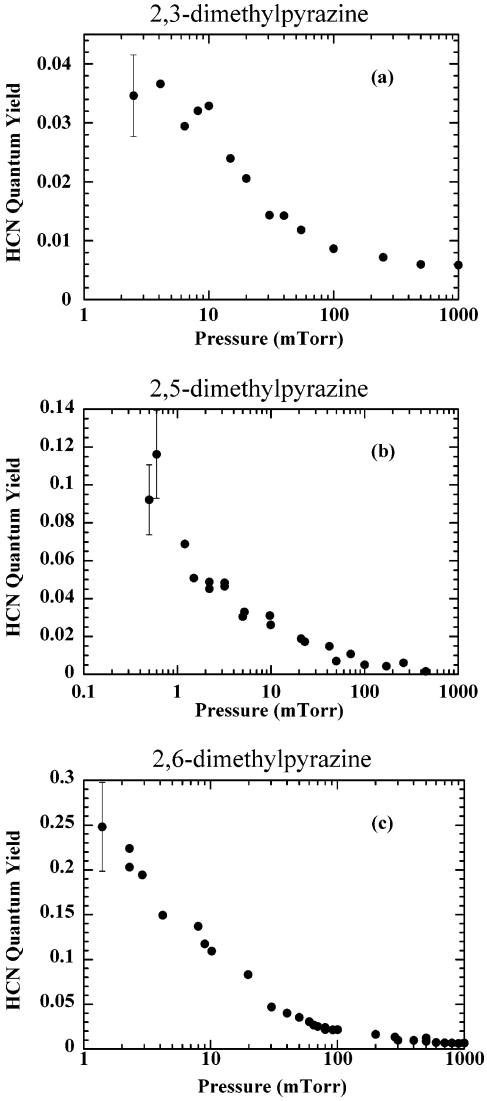

Figure 1. Quenching curves showing the HCN quantum yield dependence on pressure for the 248 nm photodissociation of (a) 2,3-dimethylpyrazine, (b) 2,5-dimethylpyrazine, and (c) 2,6-dimethylpyraizne. Displays the collisional quenching of excited dimethylpyrazine by unexcited methylpyrazine. Quantum yield measurements obtained were conducted at a UV laser fluence of 6.5, 8.4, and 4.5 mJ/cm^2 for 2,3-, 2,5-, and 2,6-dimethylpyrazine, respectively.

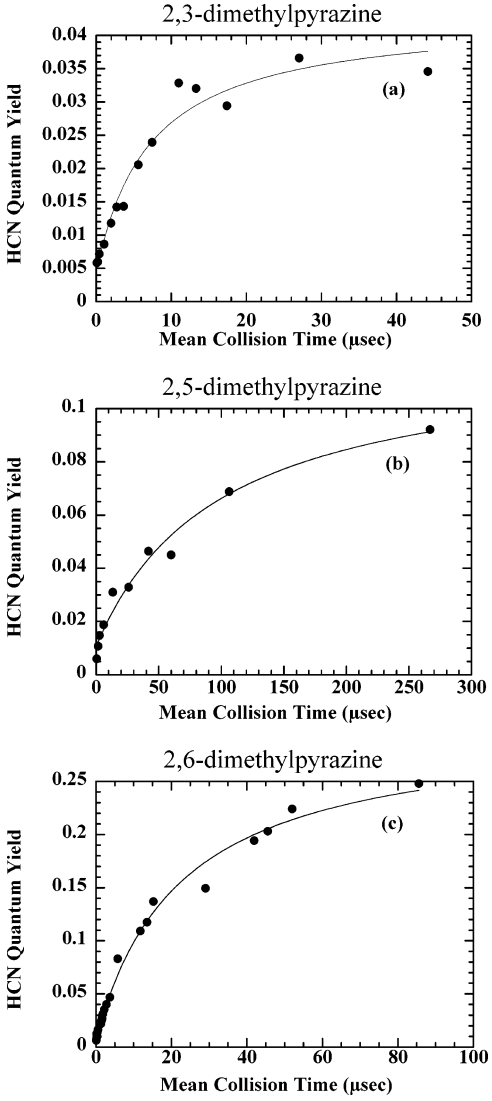

Figure 2. HCN quantum yield (ϕ) measurements displayed as a function of mean collision time produced via 248 nm excitation from (a) 2,3-dimethylpyarzine, (b) 2,5-dimethylpyrazine, and (c) 2,6-dimethylpyrazine. Mean collision times for the data sets have been calculated according to the equations shown in footnote *a* of Table 1. The circles represent the calculated HCN quantum yield, and the solid lines are the result of a three-parameter, nonlinear least-squares fit to the data using eq 11. The first-order photodissociation rate constant of 4.1×10^3, 1.0×10^3, and 1.3×10^4 s^{-1} for 2,3-, 2,5-, and 2,6-dimethylpyrazine, respectively, is determined from the results of the fit.

Baratron 220C) or 10 Torr (MKS-Baratron 222 BA) capacitance manometer, depending on the pressure range.

III. Results

A. Dimethylpyrazine Photodissociation Studies. The HCN quantum yield from 2,3-, 2,5-, and 2,6-dimethylpyrazine following 248 nm excitation has been measured as a function of dimethylpyrazine pressure. The method for calculating HCN quantum yields from the raw absorption data has been given in detail elsewhere.[54,55] Breifly, the HCN quantum yield, ϕ, from UV photodissociation is the ratio of the number of HCN molecules produced, N_{HCN}, to the number of photons absorbed, N_{abs}, or $\phi = N_{HCN}/N_{abs}$. N_{abs} is calculated according to $N_{abs} = E_{abs}(\lambda/hc)$, where E_{abs} is the total UV energy absorbed, λ is UV wavelength, h is Planck's constant, and c is the speed of light. N_{HCN} is determined by measuring IR absorption on the ν_3, P19 ($\nu = 3251.8228$ cm^{-1}) or P20 ($\nu = 3248.4839$ cm^{-1}) transition of HCN.[61] The number of HCN molecules is obtained according to $N_{HCN} = -\ln(1/(1 + |\chi|))V/\sigma l$,[62] where χ is the fractional IR absorption, V is the vacuum manifold volume consisting primarily of the cell volume with length l, and σ is the absorption cross-section for this IR transition, which is calculated from the transition line strength value, $S = 8.31$ and 6.56×10^{-20} cm^{-1} (cm^2/molecule) for P19 and P20, respectively.[61]

The dramatic decline in the HCN quantum yield from UV-excited dimethylpyrazine as a function of increasing pressure over three decades is shown in Figure 1. As has been seen with pyrazine and methylpyrazine,[52,54,55] the HCN quantum yield falls to less than half its value at the lowest pressure (~0.04, 0.12, and 0.25 for 2,3-, 2,5-, and 2,6-dimethylpyrazine, respectively), within the first decade (1−10 mTorr). The significant quenching occurring at these low pressures indicates that the photodissociation process for the dimethylpyrazines is quite slow, occurring on a microsecond time scale analogous to observations for pyrazine[52,54] and methylpyrazine.[55] Another feature of these quenching curves is that the quantum yield in the limit of high

pressure, unlike similar quenching curves for pyrazine and methylpyrazine, appears to level off to zero. Additionally, it should be pointed out that the largest value for the quantum yield, obtained at the lowest pressures, is very different for the three molecules. 2,6-Dimethylpyrazine, which has both methyl groups on either side of the same nitrogen atom, has the largest quantum yield 2−6 times the maximum value of either 2,3- or 2,5-dimethylpyrazine and about $^1/_3$rd the maximum value obtained for methylpyrazine.[55] 2,3- and 2,5-dimethylpyrazine produce a much smaller amount of HCN, even at the lowest pressures, less than $^1/_{10}$th the maximum for pyrazine and methylpyrazine previously studied.[52,54,55] The position of the methyl groups must certainly have some affect on the photodissociation reaction mechanism, which will be discussed later.

As with pyrazine[52,54] and methylpyrazine,[55] the quenching data can be used to estimate the first-order rate constant for the photoproduction of HCN and hence the lifetime of the hot parent molecule. A model that includes multiphoton ("prompt") dissociation and the possibility that two HCN molecules are formed in the photodissociation (either initially or sequentially) has been developed elsewhere[54,55] and can be used to fit the data for the three dimethylpyrazine molecules. The following kinetic scheme describes this model and serves to define the meaning of kinetic rate constants for each step. For steps that apply to all three dimethylpyrazine molecules (eqs 1−8), DMP is used as a generic term for any of the dimethylpyrazines. Kinetic steps that involve the formation of more than two products (eqs 9−10) are included for consistency with the model used to describe pyrazine and methylpyrazine photodissociation but are not necessary to fit the DMP experimental data. For these steps, 2,3-DMP is used as an example, but 2,5-, and 2,6-DMP have similar steps that lead to an identical expression for the HCN quantum yield.

$$\mathrm{DMP} + h\nu \rightarrow \mathrm{DMP}^{E'} \qquad \text{one-photon laser excitation} \qquad (1)$$

$$\mathrm{DMP}^{E'} + h\nu \rightarrow \mathrm{DMP}^{2E'} \qquad \text{multiphoton laser excitation} \qquad (2)$$

$$\mathrm{DMP}^{2E'} + \mathrm{Q} \xrightarrow{k_{qp}} \mathrm{DMP}^{2E'-\Delta E} + \mathrm{Q}^{\Delta E} \qquad \text{quenching of high-energy species} \qquad (3)$$

$$\mathrm{DMP}^{E'} + \mathrm{Q} \xrightarrow{k_{qs}} \mathrm{DMP}^{E'-\Delta E} + \mathrm{Q}^{\Delta E} \qquad \text{quenching of low-energy species} \qquad (4)$$

$$\mathrm{DMP}^{2E'} \xrightarrow{k_{d1p}} \mathrm{HCN}^* + \mathrm{C_5H_7N} \qquad \text{"prompt" dissociation} \qquad (5)$$

$$\mathrm{DMP}^{2E'} \xrightarrow{k_{d1p'}} \mathrm{CH_3CN}^* + \mathrm{C_4H_5N} \qquad \text{"prompt" dissociation} \qquad (6)$$

$$\mathrm{DMP}^{E'} \xrightarrow{k_{d1s}} \mathrm{HCN}^* + \mathrm{C_5H_7N} \qquad \text{"late" dissociation} \qquad (7)$$

$$\mathrm{DMP}^{E'} \xrightarrow{k_{d1s'}} \mathrm{CH_3CN}^* + \mathrm{C_4H_5N} \qquad \text{"late" dissociation} \qquad (8)$$

$$\text{2,3-DMP}^{E'} \xrightarrow{k_{d2s}} 2\mathrm{HCN}^* + \mathrm{CH_3CCCH_3} \qquad \text{"late" dissociation} \qquad (9)$$

$$\text{2,3-DMP}^{E'} \xrightarrow{k_{d2s'}} 2\mathrm{CH_3CN} + \mathrm{C_2H_2} \qquad \text{"late" dissociation} \qquad (10)$$

The time dependent behavior of the $\mathrm{DMP}^{E'}$, the $\mathrm{DMP}^{2E'}$, and the HCN species can be readily obtained from the differential equations describing the kinetic scheme, which at long times following dissociation can be rearranged to give

$$\phi = \left(\frac{1}{\phi_m} + \frac{t_d}{t_{coll}}\right)^{-1} + \phi_u \qquad (11)$$

Here $t_d = 1/k_s f_s$ is the effective lifetime of the excited dimethylpyrazine, $\phi_m = k_s f_s/(k_{d1s} + k_{d2s} + k_{d1s'} + k_{d2s'})$ is the maximum quantum yield from "late" dissociation, and $t_{coll} = 1/k_{qs}[Q]$ is the mean hard sphere collision time. In these terms k_s is the sum of the rate constant for the various "late" HCN dissociation channels, which for all three dimethylpyrazine molecules simplifies to

$$k_s = k_{d1s} + 2k_{d2s} \qquad (12)$$

The last term in eq 11, $\phi_u = k_{d1p} f_p/(k_{d1p} + k_{d1p'} + k_{qp}[Q])$, has been associated with "prompt", "unquenched" dissociation. Regardless of the pressure used in the present experiments, this term is not completely eliminated and is, therefore, essentially constant with respect to the collision rate ($k_{d1p} + k_{d1p'} + k_{qp}[Q] \sim k_{d1p} + k_{d1p'}$ because $k_{d1p} + k_{d1p'} \gg k_{qp}[Q]$, making $\phi_u = k_{d1p} f_p/(k_{d1p} + k_{d1p'}) = 0$ to f_p). f_p and f_s are defined as the fraction of dimethylpyrazine molecules that undergo multiphoton excitation and single photon excitation, respectively. As has been discussed elsewhere,[54] "prompt" dissociation in the pyrazine case can be associated with parent molecules having absorbed two photons as determined by studying pyrazine photochemistry as a function of photolysis laser intensity. The unimolecular rate constant associated with a species excited to 80 000 cm^{-1} is, of course, much larger than that for a species at an energy of 40 000 cm^{-1}. In these dimethylpyrazine studies, the unquenched channel is very small and an intensity dependence experiment has not been performed. We assume that the photochemistry is similar to pyrazine with the quenched channel due to single photon absorption and the very small amounts of unquenched HCN due to multiphoton absorption.[54]

Equation 11 forms the basis of a three-parameter, nonlinear least-squares fit that determines t_d, ϕ_m, and ϕ_u for each data set. Figure 2 displays the HCN quantum yield data plotted as a function of mean gas kinetic collision time and a curve representing the best fit to eq 11. Table 1 summarizes the resulting parameters, as well as k_s, the rate constant for the combined slow processes.

B. Pyrazine Photoproduct Studies. In addition to the HCN quantum yield studies for the dissociation of the DMPs, we have studied the 248 nm photodissociation of pyrazine to determine the identity of the C_3H_3N product. Although early studies[63−65] of pyrazine UV photodissociation observed a C_3H_3N product, produced with HCN, those studies did not determine the identity of the C_3H_3N product. Using FTIR we determined that the final C_3H_3N product in pyrazine 248 nm photodissociation is acrylonitrile (CH_2═CHCN). An IR spectrum of 10−20 mTorr samples of pyrazine that had first been exposed to several hundred excimer laser shots was compared to a gas-phase sample of acrylonitrile. The IR spectrum of the pyrazine photoproducts clearly identified both HCN and acrylonitrile as the photoproducts.

UV−visible spectroscopy was used to measure the UV spectrum of acrylonitrile. The spectrum indicates that acrylonitrile does not absorb in the UV range near 248. Both of these

TABLE 1: HCN Quantum Yields, Photodissociation Lifetimes, and Photodissociation Rate Constants for the 248 nm Photofragmentation of Dimethylpyrazine As Derived from Fits to the Data Shown in Figure 2 Using Eq 11[a]

molecule	ϕ_m[b]	t_d[c] (μs)	ϕ_u[d]	k_s[e] (s^{-1})
2,3-dimethylpyrazine	0.039 ± 0.007	240 ± 60	0.003 ± 0.001	4.1×10^3
2,5-dimethylpyrazine	0.14 ± 0.02	990 ± 190	0.009 ± 0.003	1.0×10^3
2,6-dimethylpyrazine	0.30 ± 0.06	76 ± 5	0.007 ± 0.002	1.3×10^4

[a] Data were collected at $I_{laser} = 9.8$, 6.6, and 7.4 mJ/cm^2 for studies of 2,3-, 2,5-, and 2,6-DMP, respectively. The fit parameters obtained from the data sets shown in Figure 2 were obtained using a hard sphere collision rate given by $k_{qs} = k_{coll} = d_{DMP}{}^2\sqrt{(8k_BT\pi/M}$, where $d_{DMP} = 5.27$ Å is the diameter of dimethylpyrazine (assumed to be equal to benzene, ref 81), k_B is Boltzmann's constant, M is the mass of dimethylpyrazine in kg, and T is the temperature of the collision cell. The mean collision time is $t_{coll} = 1/k_{coll}$[DMP]. [b] The maximum value of the HCN quantum yield. $\phi_m = k_s f_s/(k_{d1s} + k_{d2s} + k_{d1s'} + k_{d2s'})$; see text following eq 11 for definitions of symbols. [c] The photodissociation lifetime (i.e., the lifetime of vibrationally excited dimethylpyrazine) given in microseconds. $t_d = (1/k_s f_s)$; see text following eq 11 for definitions of symbols. [d] The quantum yield for the "prompt" "unquenched" channel. $\phi_u = k_{d1p}f_p/(k_{d1p} + k_{d1p'} + k_{qp}[Q]) \approx k_{d1p}f_p/(k_{d1p} + k_{d1p'}) \approx 0$ to f_p; see text following eq 11 for definitions of symbols. [e] The photodissociation rate constant given in units of s^{-1} for all the combined slow processes, $k_s = 1/t_d$.

TABLE 2: Rate Constants[a] and Maximum Quantum Yield for HCN Production via 248 nm Photodissociation of Pyrazine and Various Methyl Substituted Pyrazines and Rate Rankings[b] for Two Possible Explanations for the Trend Seen in the Rate Constants

	248 nm HCN production			
			rate rankings[b]	
molecule	k_s	ϕ_m	2,6 H atom[c] migration channel	density of states rate α $\rho^{\ddagger}/\rho$
pyrazine[d]	1.7×10^5	1.2 ± 0.2	1 (4)	1
2-methylpyrazine[e]	6.4×10^4	0.93 ± 0.08	2 (2)	2
2,3-dimethylpyrazine	4.1×10^3	0.039 ± 0.009	3 (0)	3
2,5-dimethylpyrazine	1.0×10^3	0.14 ± 0.02	3 (0)	3
2,6-dimethylpyrazine	1.3×10^4	0.30 ± 0.06	2 (2)	3

[a] Rate constants are given in units of s^{-1}. [b] Rate rankings for the proposed 2,6 H atom migration channel and density of states is a position relative to the others and not an absolute rate (i.e., 1 has the largest rate, shortest lifetime with respect to the others, and 3 has the smallest rate and the longest lifetime. [c] The numbers in parentheses represent the number of H atom migration channels that are unobstructed. [d] Pyrazine results are obtained from ref 54. [e] Methylpyrazine results are obtained from ref 55.

results related to pyrazine photochemistry will be discussed below in relation to the mechanism for pyrazine dissociation.

IV. Discussion

The lifetime of the dimethylpyrazine complexes following 248 nm excitation ranges from $t_d = 76-990$ μs, highlighting the fact that these molecules with "chemically significant" amounts of internal energy live for a very, very long time before fragmenting, even longer than pyrazine and methylpyrazine studied previously.

There are several reasons, discussed elsewhere,[55] as to why quantum yields might be less than 1. One explanation for quantum yields less than unity is that the majority of dimethylpyrazine molecules at this energy ($E \sim 40\,000$ cm^{-1}) are below the threshold for dissociation, with only a few of the excited dimethylpyrazine molecules above E_0, reflecting the thermal energy spread of initially unexcited dimethylpyrazine. Based on the pyrazine and methylpyrazine studies at 248 and 266 nm, 40 000 cm^{-1} is in the range of the dissociation threshold; however, the precise energy of the threshold in these systems is not known. Because we have probed only HCN formation in these studies, an additional explanation for less than unity HCN quantum yields is the presence of "dark" HCN channels, channels that lead to the formation of products other than HCN; any significant dark channel contributes to lowering the quantum yield for HCN. Product channels that produce acetonitrile (CH_3CN) or methylacetylene (propyne, CH_3CCH) could account in part for less than unity HCN quantum yields; however, it is likely that these channels are also dark. In addition, the dissociation lifetimes of 2,3- and 2,5-dimethylpyrazine (240 and 990 μs, respectively) are in the range of IR fluorescence lifetimes for highly vibrationally excited states. Thus, photodissociation at the lowest pressures may be in competition with radiative relaxation processes, which would lower the HCN quantum yield.[66−70] Although IR fluorescence would lead to $\phi_m < 1$, these effects are not included in the present analysis because the dimethylpyrazine IR fluorescence lifetimes are not known.

Diffusion of excited dimethylpyrazine to the walls of the cell and subsequent collisional deactivation by the cell wall prior to photodissociation would also lower quantum yields. A mean free path of 1 cm, the distance from the center of excitation volume to the cell wall, corresponds to a mean collision time of 25 μs. In all three DMP systems studied, HCN quantum yields continue to increase at times greater than 25 μs, in fact for 2,5- and 2,6-DMP the maximum quantum yield is more than twice the value at 25 μs. This indicates that wall collisions are not significantly deactivating, suggesting that highly vibrationally excited molecules may not have an efficient channel to exchange energy with the walls. Addition of a diffusion pathway[71] based on Fick's laws of mass transport to the kinetic analysis used here, confirms that wall collisions are not significantly deactivating. Assuming that vibrationally excited donor molecules are completely deactivated by collisions with the cell wall produces a fit to the data that is peaked near a mean collision time of 25 μs and then decays to zero, providing a good fit to the data at short mean collision times, before diffusion can become important, but predicting a lower quantum yield than observed at long collision times. Thus, diffusion has been ignored in our analysis both because a reasonable diffusion model does not fit the experimental results and because the addition of the model does not affect the measured rate constant, which is determined primarily by the small collision time data.

It is expected that due to the increased number of atoms and the resulting greater state density, the dimethylpyrazine molecules are expected to have longer dissociation lifetimes than

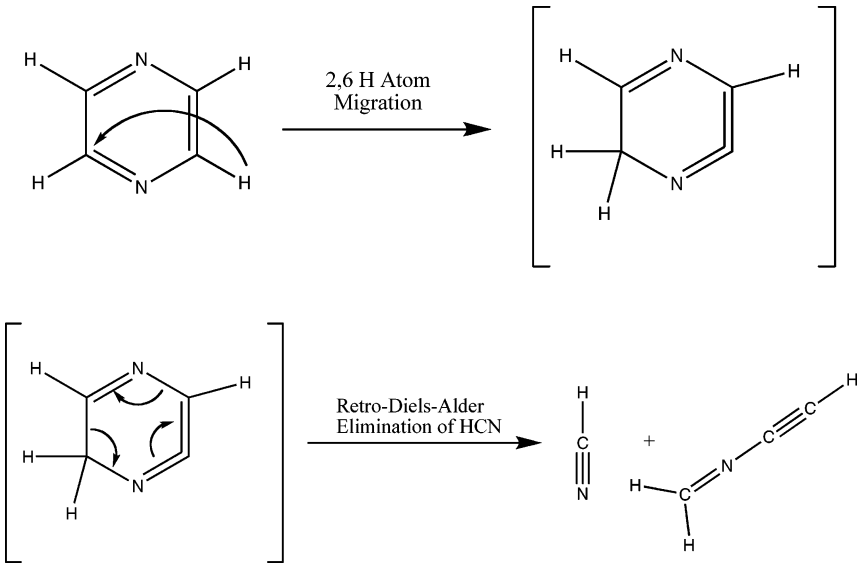

Figure 3. Pyrazine photodissociation mechanism proposed by Kiefer.[78] The first step involves a migration of a hydrogen atom from the 2 to 6 position across one of the nitrogen atoms; note that there are four possible migration channels for pyrazine and two or fewer for each of the various methylated pyrazines. The second step involves the shifting of bonds that results in ring opening in combination with a retro-Diels−Alder elimination reaction that produces HCN.

pyrazine or methylpyrazine at the same photolysis energy according to RRKM. Table 2 shows that the photodissociation rate constant for methylpyrazine[55] is about $^1/_3$rd that for pyrazine[52,54] dissociation. The rate constants for HCN formation from the dimethylpyrazines are all smaller than the methylpyrazine rate constant, as expected; however, what is not expected is that they are so different from each other. An increase in state density alone cannot account for the change in the HCN rate constant, because as noted in Table 2, the density of states for all three DMP molecules is similar; thus, if state density is the entire story, then the rate constants should be essentially the same. For 2,6-DMP, the HCN rate constant is similar in magnitude to that of methylpyrazine and the HCN quantum yield is the largest of the three DMP. The HCN rate constants for 2,3- and 2,5- are an order of magnitude smaller than 2,6-DMP and methylpyrazine. The HCN rate constant appears to be associated with the position of the methyl groups, rather than simply an increase in vibrational modes and state density. This suggests that the mechanism for pyrazine dissociation to form HCN is affected by the position of the methyl groups.

Before discussing potential dissociation reaction mechanisms for the pyrazine family of molecules, it is important to first consider the IR and UV−visible studies of pyrazine photoproducts presented above, because potential mechanisms must be consistent with these results. The FTIR spectrum of 248 nm pyrazine photoproducts indicates that acrylonitrile (CH_2CHCN) is the previously undetermined C_3H_3N product.

Although previous pyrazine photodissociation studies[54] show evidence for pyrazine multiphoton UV absorption, prompt HCN formation, and C_2H_2 formation, because the identity of the C_3H_3N product was not known, the connection between these was unclear. The identity was not critical for that work, because the kinetic scheme was independent; however, for understanding the reaction mechanism, the connection between these processes is important. UV−visible studies indicate that acrylonitrile, the additional pyrazine photodissociation product, does not absorb 248 nm radiation; therefore, the only way to obtain two HCN molecules from pyrazine photodissociation is to come from an initially excited pyrazine molecule, rather than a first HCN coming from initial pyrazine excitation followed by a second HCN resulting from UV excitation of the C_3H_3N complex. Studies of acetylene formation from pyrazine[54] indicate that the rate of C_2H_2 formation is very slow with a quantum yield essentially the same as the unquenched HCN quantum yield. This, along with the result that acrylonitrile does not absorb 248 nm, suggests that the reaction channel that produces two HCN molecules initially produces one HCN promptly, followed by a second HCN molecule and a C_2H_2 molecule that are both produced from a C_3H_3N complex with excess energy, according to

$$\text{pyrazine} + 2h\nu \rightarrow \text{pyrazine}^{2E'} \quad \text{multiphoton laser excitation} \quad (13)$$

$$\text{pyrazine}^{2E'} \xrightarrow{k_{d1p}} \text{HCN} + C_3H_3N^* \text{“prompt” dissociation} \quad (14)$$

$$C_3H_3N^* \xrightarrow{k_{d2s}} \text{HCN} + C_2H_2 \quad \text{“late” dissociation} \quad (15)$$

Although kinetic results from this alternative scheme are the same as reported previously, the pyrazine dissociation mechanism must also be consistent with this scheme.

About 40 years ago,[72−75] it was observed that 253.7 nm irradiation of pyrazine produced pyrimidine in an interchange of adjacent ring atoms. Recent computational work[76] suggests that the mechanism for this isomerization is a rotation about one of the CN bonds. Ni and co-workers[77] have recently shown that HCN and acrylonitrile are the products from one of the product channels in the 248 nm dissociation of pyrimidine. Thus it is possible that the initial step in UV dissociation of pyrazine is the CN exchange leading to pyrimidine formation followed by dissociation according the mechanism proposed by Ni to produce HCN and acrylonitrile. However, Ni and co-workers observed multiple product channels at 248 nm with the HCN/acrylonitrile channel having the highest reaction barrier. This suggests that the CN exchange is not the most likely first step in the pyrazine photodissociation mechanism.

Kiefer has suggested an alternative reaction mechanism for HCN production from UV excited pyrazine.[78] The first step of Kiefer's mechanism, shown in Figure 3, involves a hydrogen atom migration across one of the nitrogen atoms followed by bond rearrangement, and a retro-Diels−Alder type reaction. The initial step in Keifer's mechanism, the hydrogen atom migration

across a nitrogen atom, is consistent with the HCN rate constants in Table 2. For pyrazine, any of the four hydrogen atoms arefree to migrate; thus, there are four possible 2,6-H atom migration channels available to excited pyrazine molecules. For methylpyrazine, one of those channels is eliminated by the replacement of hydrogen by the methyl group and a second of those channels is sterically hindered by the methyl group. For the DMP molecules, two of the H atom migration channels are eliminated by the addition of two methyl groups; however, the number of sterically hindered migration pathways differs for the three. 2,6-DMP is similar to methylpyrazine with two unhindered pathways, but for 2,3- and 2,5-DMP all H atom pathways are hindered. These numbers are consistent with the order of magnitude of the HCN rate constant. Pyrazine has the greatest rate constant, followed by methylpyrazine and 2,6-DMP, which have rate constants of the same order of magnitude, followed by 2,3- and 2,5-DMP, which also have rate constants of the same order of magnitude. The number of open migration pathways is also consistent with the maximum quantum yield. 2,3- and 2,5-DMP both have very small maximum HCN quantum yields, whereas 2,6-DMP has a much larger maximum HCN yield.

The second step in Kiefer's mechanism, a simple ring opening, does not produce acrylonitrile as the C_3H_3N product; thus, a rearrangement of the C_3H_3N complex is necessary to produce the observed product. It has been suggested that pyrazine initially forms a bicyclic compound,[65] similar to dewar benzene, which could lead to acrylonitrile formation; however, preliminary computational work on the reaction pathway indicates that the transition state necessary to form the bicyclic compound from pyrazine is too high in energy for this pathway to be the dominate reaction channel at 40 000 cm^{-1}. An alternative to the formation of a bicyclic compound is brief formation of a four member ring, which not only would lead to the correct product in the primary pyrazine channel but also could account for the pyrazine dissociation channel that leads to the formation of two HCN molecules and acetylene.[54] As discussed below, we are currently performing additional experimental and computational studies to shed greater light on this mechanism.

As mentioned in the Introduction, energy transfer processes in which large amounts of energy are transferred in a single collision, sometimes called "supercollisions", seem to be the result of energy transfer from out-of-plane, low-frequency vibrational modes. Quantum scattering calculations of Clary et al.[27] explored the energy transfer efficiency of the vibrational modes of benzene in collisions between excited benzene molecules and He atoms. Their results indicated that only three vibrational modes, those with the smallest frequency, gave vibrational relaxation cross-sections of "appreciable magnitude". The three active modes were ν_{16} and ν_{11} (both out-of-plane vibrations) and ν_6 an in-plane antisymmetric ring stretching mode, but none of the CH stretching modes contributed to large ΔE's. Even when ν_6, the second most efficient energy transfer mode, was artificially given the same frequency as ν_{16}, the most efficient energy transfer mode, ν_6 (the in-plane mode) was still less efficient at transferring energy than ν_{16} (the out-of-plane mode). The difference in efficiency was especially apparent for larger ΔE values where the energy transfer cross-sections for ν_{16} were greater than those for ν_6 by more then an order of magnitude, even when both were given the same vibrational frequency. The quantum scattering calculations further indicate that multiquantum transitions with the ν_{16} mode had the largest energy transfer cross-sections. Thus the energy transfer cross-section was considerably larger in the calculations where the benzene molecule was initially excited with multiple quanta in low-frequency out-of-plane modes. The quantum scattering work of Clary et al. is supported by classical trajectory calculations of energy transfer from vibrationally excited CS_2 by Lendvay.[33] As was observed in the quantum scattering calculations, the lowest frequency modes were the most efficient at transferring energy; even when higher frequency modes were artificially lowered, the bend was still the most efficient energy transfer mode. Lendvay suggests that the bending mode in CS_2 is a "gateway" mode through which energy "leaks out" of the molecule.

Energy transfer calculations of Lendvay, Schatz, and Harding[28] indicate that the average energy transferred from vibrationally excited SO_2 increases linearly with E at low energies, but near dissociation the energy transfer becomes more efficient, with the dependence of ΔE on E becoming stronger than quadratic. Recent calculations[53] performed in our lab of the energy transfer probability distribution function from experimental results of Mullin[38,41,42] and Flynn[30] for the pyrazine/CO_2 indicate that it is the fraction of supercollisions, rather than the energy transfer magnitude of the collisions that increases near dissociation.

Low-frequency, out-of-plane molecular motions appear to play a role in supercollisions. As internal energy approaches the dissociation threshold, the dependence of ΔE on internal energy changes from linear to stronger than quadratic. The increase in ΔE at internal energies near threshold is due to an increase in the number of supercollisions, while the magnitude of the supercollisions remains constant; thus near the dissociation threshold, more collisions are strong. Therefore, it seems reasonable that the molecular motions involved in supercollisions (low-frequency, out-of-plane) are the same as the motions that lead to dissociation. If this is true, the dissociation mechanism should be related to these low-frequency, in particular out-of-plane, motions. In other words, the low-frequency vibrations responsible for supercollisions become even more "active" near dissociation, suggesting that these modes are related to the dissociation mechanism.

Considering only the lowest frequency pyrazine vibrational modes, those which according to Clary et al. and Lendvay should have the largest energy transfer cross-sections, it is possible to calculate the average quanta in each at $E = 40\,640$ cm^{-1}, an energy where dissociation occurs, according to[79]

$$\langle v_i \rangle = \frac{\sum_{v_i=1}^{\max} v_i \rho_{s-1}(E - v_i h\nu_i)}{\rho_s(E)} \tag{16}$$

where $\rho_s(E)$ and $\rho_{s-1}(E - v_i h\nu_i)$ are the density of states for all s vibrational oscillators at energy $E = 40\,640$ cm^{-1}, and for $s - 1$ modes omitting the ith mode and the energy of that mode, respectively. v_i is the vibrational quantum number in the ith mode, with a maximum value given by $\max = E/h\nu_i$.[79] The density of states are calculated according to the Whitten−Rabinovitch method.[80] The average energy per vibrational mode can also be calculated according to

$$\langle E_i \rangle = h\nu_i \langle v_i \rangle \tag{17}$$

Table 3 lists the nine lowest frequency modes of pyrazine (those with $\nu < 1000$ cm^{-1}) along with a description of the mode, the average quanta and vibrational energy in the mode at $E = 40\,640$ cm^{-1}, and the potential reaction mechanism

TABLE 3: Vibrational Frequencies, Mode Character, the Average Vibrational Energy, and Average Vibrational Quantum Number per Vibrational Mode at $E = 40\,640$ cm^{-1} [a] for Pyrazine Vibrational Modes Less than 1000 cm^{-1} Listed by Increasing Frequency

frequency (cm^{-1})[b]	vibrational mode[c]	mode character[d]	reaction mechanism[e]	$\langle v\rangle_i$[f]	$\langle E_{vib}\rangle_i$[g]
340	16a	out-of-plane CC bending	H-atom migration	6.20	2107
416	16b	out-of-plane CC bending	H-atom migration	4.98	2071.1
516	6b	CC antisymmetric ring stretching	4-member ring formation	3.92	2024.5
596.1	6a	CC antisymmetric ring stretching	4-member ring formation	3.33	1987.7
703	4	out-of-plane CC bending	rotation about C−N bond	2.76	1939.2
757	10a	out-of-plane CH bending	H-atom migration	2.53	1914.9
804	11	out-of-plane CH bending	H-atom migration	2.36	1894.1
918.6	5	out-of-plane CC- and CH bending	H-atom migration	2.01	1843.7
950	17a	out-of-plane CH bending	H-atom migration	1.93	1830

[a] The internal energy of pyrazine following UV excitation, $E = h\nu$ (photon energy) + E_{kT}, where E_{kT} is the thermal energy of pyrazine at $T =$ 298 K, $E_{kT} = \sum h\nu_i/[\exp(h\nu_i/kT) - 1] = 317$ cm^{-1} ($i = 0 - 24$). [b] Pyrazine vibrational frequencies obtained from reference 82. [c] Vibrational mode assignments are based on those for benzene as assigned by E. B. Wilson, Jr.,[83] which are consistent with common practice in the literature, rather than the "standard" assignments made by Herzberg[84] or Mulliken.[85] [d] Vibrational mode character descriptions based on the sketches of the benzene vibrational modes; see refs 83 and 86. [e] The pyrazine reaction mechanism step that is consistent with the vibrational motion of the mode. The H-atom migration is the first step in Kiefer's proposed mechanism, the four-member ring formation is also consistent with a dewar pyrazine, and the C−N bond rotation would lead to pyrazine to pyrimidine isomerization. [f] The average number of quanta in the vibrational mode, $\langle v_i\rangle = [\sum_{v_i=1}^{\max} v_i\rho_{s-1}(E - v_ih\nu_i)]/\rho_s(E)$, where $\rho_s(E)$ and $\rho_{s-1}(E - v_ih\nu_i)$ are the density of states for all s vibrational oscillators at energy E, and for $s - 1$ modes omitting the ith mode and the energy of that mode. v_i is the vibrational quantum number in the ith mode, with a maximum value given by max $= E/h\nu_i$.[79] The density of states are calculated according to the Whitten-Rabinovitch method.[80] [g] The average vibrational energy per mode, $\langle E_i\rangle = h\nu_i\langle v_i\rangle$.[79]

process consistent with the motion. Of the nine lowest frequency pyrazine modes, seven have out-of-plane motion. Five of those seven modes have a motion that is consistent with the H atom migration step proposed by Kiefer, and only one has a motion consistent with the pyrazine to pyrimidine isomerization. The two in-plane ring-stretching modes are consistent either with a four-membered ring formation or with the bicyclic dewar pyrazine formation. It should also be noted that five of these modes (ν_{16a}, ν_{16b}, ν_{6a}, ν_{6b}, and ν_{11}) have the same motion as those that Clary et al.[27] determined were the most efficient in benzene to He energy transfer. These modes are, on average, excited with a large number of quanta at this energy, again consistent with the requirements for efficiency given by the quantum scattering calculations. The calculations in Table 3 support the theory that the molecular motions that lead to supercollisions (low-frequency, particularly out-of-plane motions) are the same motions that lead to dissociation. The proposed reaction mechanism is consistent with these same molecular motions. Thus the significant increase in energy transfer efficiency near threshold seems to be the result of increased excitation in the modes responsible for supercollisions, which are the modes that couple into the reaction coordinate for the dissociation process.

Several experiments are currently underway in our lab to more fully understand pyrazine photochemistry and its relation to energy transfer. These experiments include classical quenching studies of pyrazine-d_4 to determine if changes to the rate constant are consistent with the H-atom migration step, time-resolved step-scan FTIR to observe intermediates in the reaction mechanism, and computational work to calculate the potential energy along proposed reaction pathways.

V. Conclusion

The work described in this paper provides insight into the dissociation of highly vibrationally excited 2,3-, 2,5-, and 2,6-dimethylpyrazine following the absorption of UV laser radiation. Additionally, the C_3H_3N 248 nm pyrazine photoproduct has been identified as acrylonitrile using IR spectroscopy. These results, together with previously obtained photofragmentation studies of UV excited pyrazine[51,52,54] and methylpyrazine,[55] are used to explore possible dissociation mechanisms for the pyrazine family of molecules, as well as the relationship between molecular motions that lead to dissociation and the motions that lead to large energy transfer events. The HCN quantum yield was measured using high-resolution IR diode probing of the HCN photoproduct as a function of quencher gas pressure, and a hard sphere gas kinetic collision model was employed to determine the time scale of the dissociation process (240 ± 60 μs, 990 ± 190 μs, and 76 ± 5 μs for 2,3-, 2,5-, and 2,6-dimethylpyrazine, respectively).

The position of the methyl group affects the HCN rate constant, suggesting that the mechanism for dissociation involves a step that is hindered by the addition of the methyl groups. The proposed initial molecular motions of the mechanism, an out-of-plane H atom migration across a N atom, is consistent with the position of the methyl groups and the dissociation lifetime of the various pyrazine molecules studied. This mechanism is also consistent with the large energy transfer magnitudes observed near dissociation when collisions involving highly excited pyrazine are studied. These so-called "supercollisions" have been linked to low-frequency out-of-plane motion. This suggests that the molecular motions leading to efficient energy transfer are the same motions involved in dissociation. Experiments are currently underway in our lab to more fully understand pyrazine photochemistry and its relation to energy transfer.

Acknowledgment. This work was performed at Brigham Young University and Columbia University, and supported by the Department of Energy (DE-FG02-88ER13937). Equipment support was provided by the National Science Foundation (CHE-97-27205) and the Joint Services Electronics Program (U.S. Army, U.S. Navy, and U.S. Air Force; DAAH04-94-G-0057). E.T.S. acknowledges George W. Flynn of Columbia University for use of equipment and laboratory space. A.M.D. and J.A.J. acknowledge support from the BYU ORCA fellowship program and the BYU Department of Chemistry and Biochemistry Undergraduate Research Awards program. M.A.M. acknowledges sabbatical support from Calvin College and the Calvin College-Howard Hughes Medical Institute Grant.

References and Notes

(1) Gilbert, R. G.; Smith, S. C. *Theory of Unimolecular and Recombination Reactions*; Blackwell Scientific Publications: Oxford, U.K., 1990.

(2) Lindemann, F. A. *Trans. Faraday Soc.* **1922**, *17*, 598.
(3) Michaels, C. A.; Flynn, G. W. *J. Chem. Phys.* **1997**, *106*, 3558.
(4) Lenzer, T.; Luther, K.; Reihs, K.; Symonds, A. C. *J. Chem. Phys.* **2000**, *112*, 4090.
(5) Grigoleit, U.; Lenzer, T.; Luther, K.; Mutzel, M.; Takahara, A. *Phys. Chem. Chem. Phys.* **2001**, *3*, 2191.
(6) Nilsson, D.; Nordholm, S. *J. Chem. Phys.* **2002**, *116*, 7040.
(7) Nilsson, D.; Nordholm, S. *J. Chem. Phys.* **2003**, *119*, 11212.
(8) Hold, U.; Lenzer, T.; Luther, K.; Symonds, A. C. *J. Chem. Phys.* **2003**, *119*, 11192.
(9) Lenzer, T.; Luther, K.; Nilsson, D.; Nordholm, S. *J. Phys. Chem. B* **2005**, *109*, 8325.
(10) Hsu, H. C.; Liu, C.-L.; Lyu, J.-J.; Ni, C.-K. *J. Chem. Phys.* **2006**, *124*, 134303.
(11) Liu, C.-L.; Hsu, H.-C.; Lyu, J.-J.; Ni, C.-K. *J. Chem. Phys.* **2006**, *124*, 054302.
(12) Liu, C.-L.; Hsu, Hsu, C.; Lyu, J.-J.; Ni, C.-K. *J. Chem. Phys.* **2006**, *125*, 204309.
(13) Michaels, C. A.; Lin, Z.; Mullin, A. S.; Tapalian, H. C.; Flynn, G. W. *J. Chem. Phys.* **1996**, *106*, 7055.
(14) Sevy, E. T.; Rubin, S. M.; Lin, Z.; Flynn, G. W. *J. Chem. Phys.* **2000**, *113*, 4912.
(15) Liu, C.-L.; Hsu Hsu, C.; Lyu, J.-J.; Ni, C.-K. *J. Chem. Phys.* **2005**, *123*, 131102.
(16) Brown, N. J.; Miller, J. A. *J. Chem. Phys.* **1984**, *80*, 5568.
(17) Hassoon, S.; Oref, I.; Steel, C. *J. Chem. Phys.* **1988**, *89*, 1743.
(18) Löhmannsröben, H. G.; Luther, K. *Chem. Phys. Lett.* **1988**, *144*, 473.
(19) Luther, K.; Reihs, K. *Ber. Bunsenges. Phys. Chem.* **1988**, *92*, 442.
(20) Morgulis, J. M.; Sapers, S. S.; Steel, C.; Oref, I. *J. Chem. Phys.* **1989**, *90*, 923.
(21) Lendvay, G.; Schatz, G. C. *J. Phys. Chem.* **1990**, *94*, 8864.
(22) Clarke, D. L.; Thompson, K. C.; Gilbert, R. G. *Chem. Phys. Lett.* **1991**, *182*, 357.
(23) Bernshtein, V.; Oref, I. *J. Phys. Chem.* **1993**, *97*, 12811.
(24) Mullin, A. S.; Park, J.; Chou, J. Z.; Flynn, G. W.; Weston, R. E., Jr. *Chem. Phys.* **1993**, *175*, 53.
(25) Bollati, R. A.; Ferrero, J. C. *Chem. Phys. Lett.* **1994**, *218*, 159.
(26) Bollati, R. A.; Ferrero, J. C. *J. Phys. Chem.* **1994**, *98*, 3933.
(27) Clary, D. C.; Gilbert, R. G.; Bernshtein, V.; Oref, I. *Faraday Discuss.* **1995**, *102*, 423.
(28) Lendvay, G.; Schatz, G. C.; Harding, L. B. *Faraday Discuss.* **1995**, *102*, 389.
(29) Oref, I. Supercollisions. In *Advances in Chemical Kinetics and Dynamics: Vibrational Energy Transfer Involving Large and Small Molecules*; Barker, J. R., Ed.; JAI Press Inc.: Greenwich, CT, 1995; Vol. 2B, pp 285.
(30) Mullin, A. S.; Michaels, C. A.; Flynn, G. W. *J. Chem. Phys.* **1995**, *102*, 6032.
(31) Thomas, L.; Klaus, L.; Jurgen, T.; Robert, G. G.; Kieran, F. L. *J. Chem. Phys.* **1995**, *103*, 626.
(32) Bernshtein, V.; Oref, I. The contribution of wide-angle motions to collisional energy transfer between benzene and argon. In *Highly Excited Molecules: Relaxation, Reaction, and Structure*; Mullin, A. S., Schatz, G. C., Eds.; American Chemical Society: Washington, DC, 1997; Vol. 678, pp 251.
(33) Lendvay, G. *J. Phys. Chem. A* **1997**, *101*, 9217.
(34) Johnson, J. A.; Duffin, A. M.; Hom, B. J.; Jackson, K. E.; Johnson, J. A.; Sevy, E. T. *J. Chem. Phys.*, in press.
(35) Johnson, J. A.; Kim, K.; Mayhew, M.; Mitchell, D. G.; Sevy, E. T. *J. Phys. Chem. A*, submitted for publication.
(36) Fraelich, M.; Elioff, M. S.; Mullin, A. S. *J. Phys. Chem. A* **1998**, *102*, 9761.
(37) Wall, M. C.; Lemoff, A. S.; Mullin, A. S. *J. Phys. Chem. A* **1998**, *102*, 9101.
(38) Wall, M. C.; Mullin, A. S. *J. Chem. Phys.* **1998**, *108*, 9658.
(39) Wall, M. C.; Stewart, B. A.; Mullin, A. S. *J. Chem. Phys.* **1998**, *108*, 6185.
(40) Elioff, M. S.; Fraelich, M.; Sansom, R. L.; Mullin, A. S. *J. Chem. Phys.* **1999**, *111*, 3517.
(41) Elioff, M. S.; Wall, M. C.; Lemoff, A. S.; Mullin, A. S. *J. Chem. Phys.* **1999**, *110*, 5578.
(42) Wall, M. C.; Lemoff, A. S.; Mullin, A. S. *J. Chem. Phys.* **1999**, *111*, 7373.
(43) Elioff, M. S.; Sansom, R. L.; Mullin, A. S. *J. Phys. Chem. A* **2000**, *104*, 10304.
(44) Elioff, M. S.; Fang, M.; Mullin, A. S. *J. Chem. Phys.* **2001**, *115*, 6990.
(45) Park, J.; Li, Z.; Lemoff, A. S.; Rossi, C.; Elioff, M. S.; Mullin, A. S. *J. Phys. Chem. A* **2002**, *106*, 3642.
(46) Park, J.; Shum, L.; Lemoff, A. S.; Werner, K.; Mullin, A. S. *J. Chem. Phys.* **2002**, *117*, 5221.
(47) Li, Z.; Korobkova, E.; Werner, K.; Shum, L.; Mullin, A. S. *J. Chem. Phys.* **2005**, *123*, 174306/1.
(48) Li, Z.; Sansom, R.; Bonella, S.; Coker, D. F.; Mullin, A. S. *J. Phys. Chem. A* **2005**, *109*, 7657.
(49) Miller, E. M.; Murat, L.; Bennette, N.; Hayes, M.; Mullin, A. S. *J. Phys. Chem. A* **2006**, *110*, 3266.
(50) Havey, D. K.; Liu, Q.; Li, Z.; Elioff, M.; Fang, M.; Neudel, J.; Mullin, A. S. *J. Phys. Chem. A* **2007**, *111*, 2458.
(51) Sevy, E. T.; Michaels, C. A.; Tapalian, H. C.; Flynn, G. W. *J. Chem. Phys.* **2000**, *112*, 5844.
(52) Michaels, C. A.; Tapalian, H. C.; Lin, Z.; Sevy, E. T.; Flynn, G. W. *Faraday Discuss.* **1995**, *102*, 405.
(53) Hom, B. J.; Sevy, E. T. Manuscript in preparation.
(54) Sevy, E. T.; Muyskens, M. A.; Rubin, S. M.; Flynn, G. W.; Muckerman, J. T. *J. Chem. Phys.* **2000**, *112*, 5829.
(55) Sevy, E. T.; Muyskens, M. A.; Lin, Z.; Flynn, G. W. *J. Phys. Chem. A* **2000**, *104*, 10538.
(56) Flynn, G. W.; Weston, R. E., Jr. *J. Phys. Chem.* **1993**, *97*, 8116.
(57) Michaels, C. A.; Mullin, A. S.; Flynn, G. W. *J. Chem. Phys.* **1995**, *102*, 6682.
(58) Ondrey, G. S.; Bersohn, R. *J. Chem. Phys.* **1984**, *81*, 4517.
(59) Goates, S. R.; Chu, J. O.; Flynn, G. W. *J. Chem. Phys.* **1984**, *81*, 4521.
(60) Muyskens, M. A.; Sevy, E. T. *J. Chem. Educ.* **1997**, *74*, 1138.
(61) Rothman, L. S.; Gamache, R. R.; Barbe, A.; Goldman, A.; Gillis, J. R.; Brown, L. R.; Toth, R. A.; Flaud, J. M.; Camy-Peyret, C. *Appl. Opt.* **1983**, *22*, 2247.
(62) Pugh, L. A.; Rao, K. N. Intensities from infrared spectra. In *Molecular Spectroscopy: Modern Research Volume II*; Rao, K. N., Ed.; Academic Press: New York, 1976; pp 165.
(63) Chesko, J. D.; Lee, Y. T. Unimolecular Decay of Azabenzene: A Mechanistic Model Based on Pyrazine's Photoreactive Relaxation Pathways. In *Highly Excited Molecules: Relaxation, Reaction, and Structure*; Mullin, A. S., Schatz, G. C., Eds.; American Chemical Society: Washington, DC, 1997; Vol. 678, pp 107.
(64) Chesko, J. D.; Stranges, D.; Suits, A. G.; Lee, Y. T. *J. Chem. Phys.* **1995**, *103*, 6290.
(65) Chesko, J. D. M. Quantum Symmetry and Photoreactivity of Azabenzenes. Ph.D. Dissertation, University of California, 1995.
(66) Barker, J. R.; Brenner, J. D.; Toselli, B. M. The Vibrational Deactivation of Large Molecules by Collisions and by Spontaneous Infrared Emission. In *Advances in Chemical Kinetics and Dynamics: Vibrational Energy Transfer Involving Large and Small Molecules*; Barker, J. R., Ed.; JAI Press Inc.: Greenwich, CT, 1995; Vol. 2B, pp 393.
(67) Bevilacqua, T. J.; Andrews, B. K.; Stout, J. E.; Weisman, R. B. *J. Chem. Phys.* **1990**, *92*, 4627.
(68) Bevilacqua, T. J.; Weisman, R. B. *J. Chem. Phys.* **1993**, *98*, 6316.
(69) McDonald, D. B.; Rice, S. A. *J. Chem. Phys.* **1981**, *74*, 4907.
(70) Yamazaki, I.; Murao, T.; Yamanaka, T.; Yoshisara, K. *Faraday Discuss. Chem. Soc.* **1983**, *75*, 395.
(71) O'Neill, J. A.; Wang, C. X.; Cai, J. Y.; Flynn, G. W.; Weston, R. E. J. *J. Chem. Phys.* **1988**, *88*, 6240.
(72) Lahmani, F.; Ivanoff, N.; Magat, M. *C. R. Seances Acad. Sci., Ser. C* **1966**, *263*, 1005.
(73) Lahmani, F.; Ivanoff, N. *J. Phys. Chem.* **1972**, *76*, 2245.
(74) Lahmani, F.; Ivanoff, N. *Tetrahedron Lett.* **1967**, 3913.
(75) Lablache-Combier, A. In *Photochemistry of Heterocyclic Compounds*; Wiley: New York, 1976.
(76) Su, M.-D. *J. Phys. Chem. A* **2006**, *110*, 9420.
(77) Lin, M.-F.; Dyakov, Y. A.; Tseng, C.-M.; Mebel, A. M.; Lin, S. H.; Lee, Y. T.; Ni, C.-K. *J. Chem. Phys.* **2006**, *124*, 84303.
(78) Kiefer, J. Retro Diels Alder reaction mechanism for pyrazine, personal communication from G. W. Flynn.
(79) Durana, J. F.; McDonald, J. D. *J. Chem. Phys.* **1976**, *64*, 2518.
(80) Whitten, G. Z.; Rabinovitch, B. S. *J. Chem. Phys.* **1963**, *38*, 2466.
(81) Hirschfelder, J. O.; Curtiss, C. F.; Bird, R. B. *Molecular Theory of Gases and Liquids*; John Wiley & Sons, Inc.: New York, 1954.
(82) Simmons, J. D.; Innes, K. K. *J. Mol. Spectrosc.* **1964**, *14*, 190.
(83) Wilson, E. B., Jr. *Phys. Rev.* **1934**, *45*, 706.
(84) Herzberg, G. *Molecular Spectra and Molecular Structure II. Infrared and Raman Spectra of Polyatomic Molecules*; Van Nostrand Reinhold Company: New York, 1954.
(85) Mulliken, R. S. *J. Chem. Phys.* **1955**, *23*, 1997.
(86) Lord, R. C.; Marston, A. L.; Miller, F. A. *Spectrochim. Acta* **1957**, *9*, 113.